A 3D CFD model analysis of the hydraulics of an outfall structure at a power plant

Liaqat A. Khan, Edward A. Wicklein and Mizan Rashid

ABSTRACT

A practical application of a three-dimensional (3D) computational fluid dynamics (CFD) model to an outfall structure of a power plant is presented in this paper. The outfall structure, used for discharging 55 m^3/s of cooling water to a reservoir, consists of two inflow pipes, two deflectors and a baffle wall. The computational grid, resolving all the geometric features of the outfall structure consists of 350,660 hexahedral cells. The CFD model was run for two configurations of the outfall structure, with and without a baffle wall. The interactions of two high velocity jets with deflectors and baffle wall create complex velocity distribution and circulation patterns. Initially, both the jets bifurcate and then merge as they propagate downstream. At the outlet, the maximum near-surface velocities are not significantly different for the two configurations of the outfall structure. However, when the baffle wall is used the near-bed velocities, responsible for reservoir bed scouring, are approximately 75% smaller.

Key words | Baffles and deflectors, computational fluid dynamics, computational grid, computational hydraulics, outfall structure hydraulics

Liaqat A. Khan (corresponding author)
Edward A. Wicklein
Mizan Rashid
ENSR International,
9521 Willows Road NE, Redmond,
WA 98052, USA

INTRODUCTION

Cooling waters from thermal power plants are generally discharged back into rivers or reservoirs through outfall diffusers. Occasionally, when the water temperature is not significantly different from the ambient conditions, cooling water could be directly discharged into the receiving water body through an outfall structure. Two important features of such outfall structures are deflectors and baffle walls. The primary objectives of deflectors and baffle walls are to dissipate energy and minimize river or reservoir bed scouring. The interaction of high velocity inflow with the deflectors and baffle walls can create complex, three-dimensional flow fields in the outfall structure as well as in the adjoining reservoirs.

A 3D CFD model of an outfall structure is presented in this paper. The objectives are to analyze the flow field and investigate the design of the outfall structure in creating a uniform flow field at the outlet. Results of the CFD model with and without a baffle wall are compared to demonstrate their influence in reducing near-bed velocities at the outlet. Similar CFD models are increasingly being used in hydraulic engineering for simulating fluid–structure interactions and for optimizing the design of hydraulic structures. In the context of the current study, two reviews of CFD models can be found in Lai *et al.* (2003) and Khan *et al.* (2004).

In this study, a commercially available CFD software package is used for investigating the outfall hydraulics. An advantage of using commercial software packages (STAR-CD, FLUENT, CFX or Flow3D) is that these codes have been extensively tested and verified. These software packages utilize second- or higher-order turbulence closure schemes and do not contain arbitrary calibration coefficients, except for roughness heights. The coefficients in the turbulence models are considered global (Rodi 1980) and cannot be changed arbitrarily to match field data. For the application presented in this study, the outlet structure is made of concrete and roughness height is a known parameter. Therefore, a sufficiently refined computational

grid, with appropriate boundary conditions, is expected to provide reasonably accurate solutions for evaluating alternative designs of the outfall structure.

The above observation about commercial CFD packages is based on the large number of successful applications of these models, without making changes to codes. Some recent applications of commercial CFD software packages to hydraulic problems can be found in Brouckaert & Buckley (1999), Savage & Johnson (2001), Wright & Hargreaves (2001), Yeung (2001), Ali & Karim (2002), Greene *et al.* (2002), Morvan *et al.* (2002), Khan *et al.* (2004), Salaheldin *et al.* (2004) and Stamou (2002). Additional publications from various branches of engineering can be found at the web sites of the respective CFD software packages. Recently, Salaheldin *et al.* (2004) have used FLUENT in their study and noted "that a robust 3D hydrodynamic model can effectively supplement experimental studies in understanding the complex flow field" in hydraulic structures.

OUTFALL STRUCTURE

The salient features of the outfall structure are shown in Figure 1. In this figure, the left wall has been removed in order to visualize the interior details. The outfall structure consists of two 2.9 m diameter inflow pipes conveying 55 m^3/s of cooling water. Two deflectors, each made of a 2.1 m radius quarter cylinder, are located immediately in front of the inflow pipes. A 0.76 m wide baffle wall, across the complete width of the structure, is located at a distance of 15 m. The baffle wall is made of 4.25 m long and 0.25 m high open slots.

The length and width of the outfall structure are 23.2 m and 16.5 m, respectively. At the upstream side, the structure is divided into four bays by 1 m thick walls. The inflow pipes and deflectors are located in the left bays that are 3.8 m wide. Upstream of the baffle wall, the bed elevation is 11.75 m. Immediately after the baffle wall, the bed rises vertically by 0.3 m. Thereafter, two 1 m long humps increase the bed elevation to 13.1 m. The top elevation of the structure, as shown in Figure 1, is 17.4 m. This elevation corresponds to a low water level in the receiving water body.

COMPUTATIONAL GRID

One of the most important steps in applying a commercially available CFD software to a hydraulic problem is to develop a computational grid with adequate grid resolution. The computational grid of the outfall structure, shown in Figure 2, consists of 350,660 hexahedral cells. The number of cells along the length (excluding inflow pipes), width and height of the structure are 119, 69 and 58, respectively. The geometry of each deflector is represented by $18 \times 18 \times 16$ cells along the length, height and width, respectively. Three cells are used to resolve the height of each open slot in the baffle wall. The same number of cells is used to represent the solid area between adjacent slots. When the CFD model is run without the baffle wall, these solid elements are replaced by fluid cells. The outfall structure discharges water into a large reservoir, which is about 600 m wide and 1000 m long. The complete CFD model incorporates the reservoir with 1.25 million computational cells. As the focus of this paper is the hydraulics of the outfall structure, details of the CFD model for the reservoir are not discussed.

A critical factor determining the accuracy and convergence of a CFD model is the mesh quality (Thomson *et al.* 1999). The parameters commonly used to indicate mesh quality are determinant of cells, aspect ratio, internal angle and cell face warpage. Ideal values of the first two parameters are unity, while the later parameters should be 90° and 0°, respectively. However, these constraints cannot be satisfied when dealing with complex geometries. Therefore, commercial CFD software packages, using a finite volume method for discretizing the governing equations, allow for significant deviations for the ideal conditions. For the computational grid shown in Figure 2, the determinants of all the cells exceed 0.5, except for about 0.1% of the cells. The internal angles of all the cells are higher than 45°, while warpage of cell faces is less than 15°. Except for about 1.5% of cells, the aspect ratios of the cells are less than 10. The minimum and maximum lengths of cells in the complete model domain are 0.05 m and 0.28 m, respectively. In general, cells are smaller in the vertical as well as in the areas encompassing the deflectors and the baffle wall.

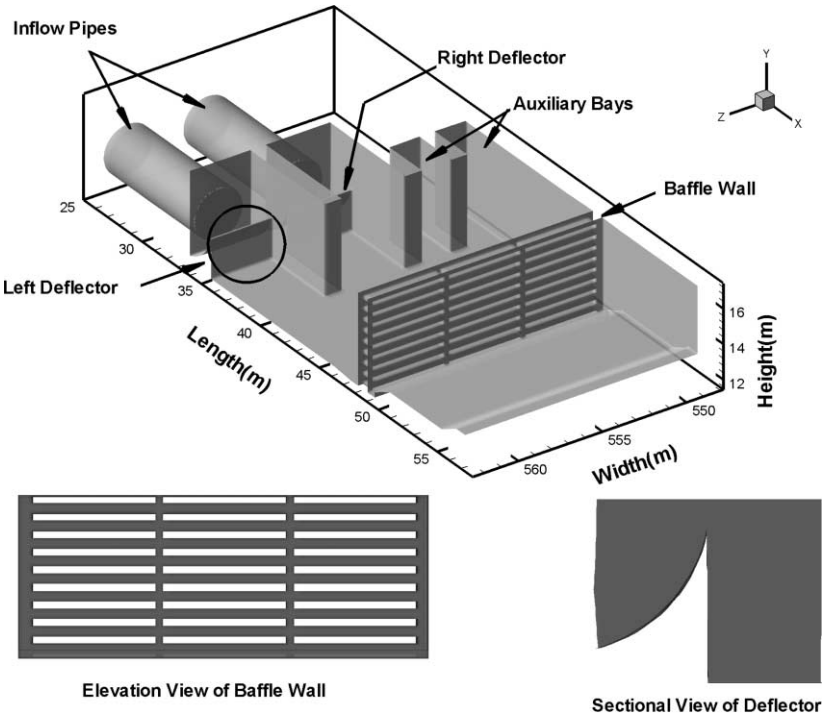

Figure 1 | Geometric features of the outfall structure used for discharging cooling water to a reservoir. The bottom panels show close-up views of a baffle wall (left) and the deflector (right).

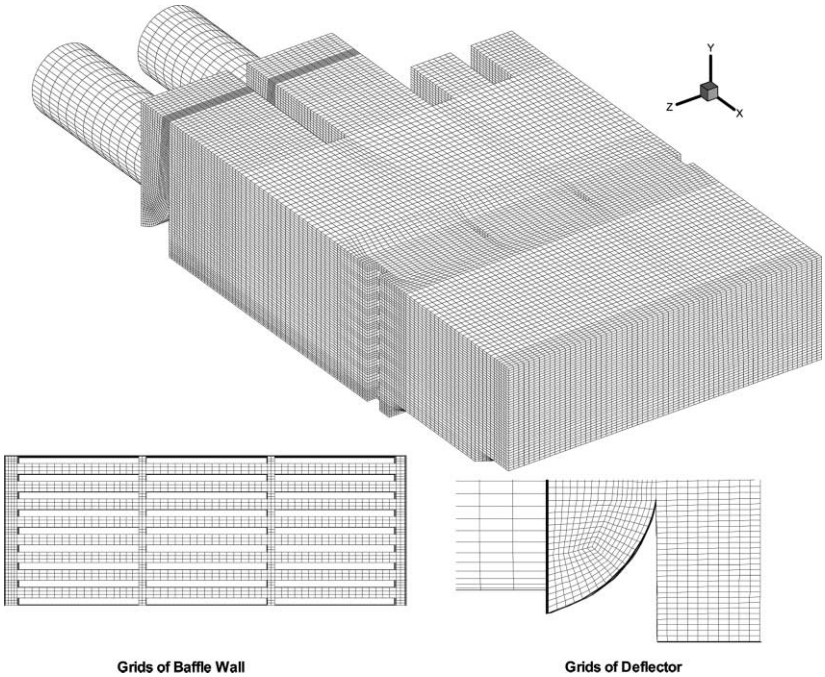

Figure 2 | Computational grid of the outfall structure. The computational grid consists of 350,660 hexahedral cells. Close-up view of computational cells of the baffle wall and the deflectors are shown in the bottom panels.

DESCRIPTION OF CFD SOFTWARE

STAR-CD (Computational Dynamics Ltd. 1999) is a commercially available CFD software that was used for simulating the flow field in the outfall structure. STAR-CD, like other CFD software packages, solves the fundamental equations for fluid flow, conservation of mass and momentum, known as the Reynolds-averaged Navier–Stokes (RANS) equations. The software solves additional equations representing turbulence characteristics ($k-\varepsilon$) to determine eddy viscosity and mixing coefficients. STAR-CD discretizes the partial differential equations by a finite-volume method and solves the resulting algebraic equations by implicit methods. The governing equations of the CFD model and the details of numerical procedures are described in Computational Dynamics Ltd. (1999). These information can also be found in Rodi (1980) and Lomax *et al.* (2003). Therefore, additional details of the CFD software are not presented in this paper.

BOUNDARY CONDITIONS

To simulate flow in the outfall structure, an inlet boundary condition (inflow velocity of 1.25 m/s) was applied at the outer face of the inflow pipes shown in Figure 1. A symmetry boundary condition was applied at the water surface. At a symmetry boundary, the velocity normal to the surface and the gradients of the dependent variables are zero. The downstream boundary is located at the far end of the reservoir, about 1000 m from the outfall structure. A pressure boundary condition was specified at the downstream boundary. At a pressure boundary, the CFD model determines velocities based on local pressure gradient and the conservation of mass and momentum. At all other surfaces, a no-slip (zero tangential and normal velocities) boundary condition was enforced by a two-point wall function approach.

With these boundary conditions, the iterative solution procedure was continued till the non-dimensional residuals of the velocity components, turbulent kinetic energy and dissipation, and mass decayed by three orders of magnitude (0.001). The resulting solution was assumed to represent the steady state velocity distribution in the model domain. The model was found to converge to steady state in less than 600 iterations, which is an indication of the high quality of the computational grid discussed earlier.

SENSITIVITY ANALYSES

During this study, a coarser grid (165,872 cells) model of the outfall structure was also developed. The differences in the computed velocities by the two CFD models were negligible. The computed results indicated the adequacy of the finer grid model, shown in Figure 2, in resolving the geometric and hydraulic features of the outfall structure. This is consistent with results of grid sensitivity analysis presented by Lai *et al.* (2003). Once a sufficiently refined grid has been defined, further improvements in the computed results with grid refinements are very small, as represented by computed velocities using MEDIUM and FINE grids by Lai *et al.* (2003).

After establishing the adequacy of the computational grid, the effects of wall roughness on the computed velocity distributions were analyzed. Initially, a wall roughness height corresponding to concrete was used in the model simulation. Then, the roughness height was increased by 50%. The computed results indicated that, in general, higher roughness decreased the computed velocities very close to the walls. However, minimal large-scale effects were apparent. Therefore, it was concluded that the wall roughness was not the dominant parameter determining the velocity distribution in the outfall structure. For a steady state problem, the geometry and the boundary conditions govern the large scale circulation pattern in the model domain. The two-point wall function method, with standard roughness height, has been found suitable for a large class of hydraulic applications, as represented by the works of Lai *et al.* (2003) and Khan *et al.* (2004). The papers cited in Lai *et al.* (2003) and Khan *et al.* (2004) provide further examples of the successful use of the standard wall approach in simulating flow fields in hydraulic engineering.

MODEL RESULTS AND ANALYSES

The results of a CFD model with and without the baffle wall are compared in Figures 3–6. Figure 3 provides overviews

of 3D velocity distributions and circulation patterns in the complete model domain. In Figures 4–6, the left panels (a, b and c) show velocity distributions with the baffle wall, while the panels on the right (d, e and f) present the corresponding information without the baffle. Velocity distributions and streamlines in three vertical sections, through the middle of the left and right deflectors and the left auxiliary bay, are shown in Figure 4. The corresponding information in three horizontal planes, at different elevations, are presented in Figure 5. These sections are located just above the deflector (a and d), approximately at mid-depth (b and e) and near the water surface (c and f). The velocity distributions in three transverse sections, immediately downstream of the deflector (a and d), through the baffle wall position (b and e) and at the outlet (c and f), are shown in Figure 6. As the structure extends into the reservoir through the adjacent embankments, all the panels in Figure 5 and the bottom panels in Figure 6 include regions of the reservoir.

Many of the flow features described in this section can be observed in Figure 3. The complex circulation patterns

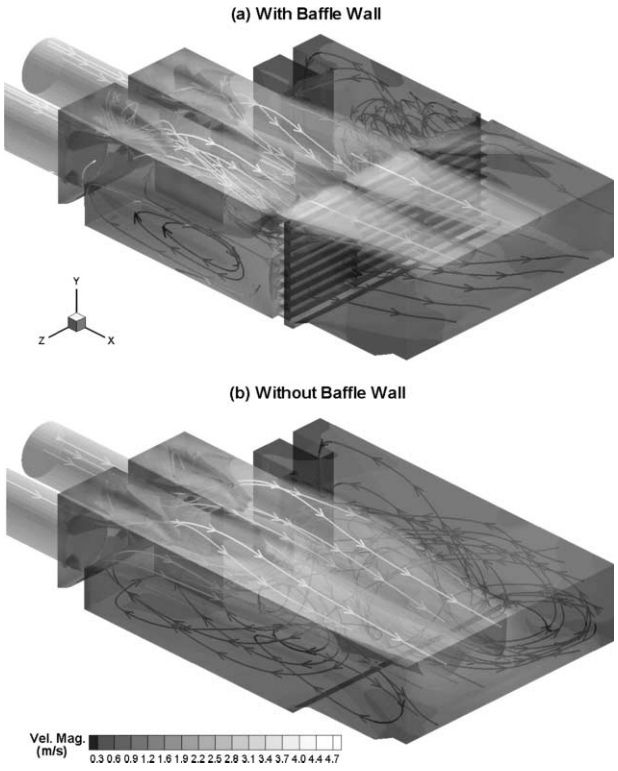

Figure 3 | Overview of 3D velocity field in the outfall structure for two configurations: a) with baffle wall and b) without baffle wall.

are indicated by the streamlines. The deflectors create high velocity jets, which rise towards the water surface and become horizontal at a distance of about 10 m from the deflectors (Figures 4(a), (b), (d) and (f)). The highest velocity inside the jet is approximately 5 m/s, which is significantly higher than the average velocity (1.25 m/s) in the inflow pipes. An interesting feature of the jets is their bifurcation with increase in elevation (Figures 5(c) and (f) and Figures 6(a) and (d)). As the jets travel downstream, they spread out laterally (Figures 5(b), (c), (e) and (f)) and become quite thin near the water surface (Figures 4(a), (b), (d) and (f)). The shear stresses exerted by the jets on the surrounding water create eddies, dead flow zones and flow separations.

With the baffle wall in place, the circulation patterns in front of the two deflectors are quite similar (Figures 4(a) and (b) and Figures 5(a) and (b)). Large eddies develop below the high velocity jet, with downwelling from the upper water column. At the baffle wall, velocities are relatively higher in the upper water column. Downstream of the baffle wall, velocity distributions are quite different, especially towards the outlet. An eddy forms at the downstream of the right deflector (Figure 4(a)), which forces most of the outflow through the upper water column. The outflow is relatively uniform in the section through the left deflector (Figure 4(b)), as indicated by essentially parallel streamlines.

Without the baffle walls, circulation patterns in sections through the left and right deflectors are quite different (Figures 4(d) and (e)). The eddy in front of the left deflector is larger and extends to the downstream end of the outfall structure. The hump in the structure bed keeps the center of the eddy from moving into the reservoir. The center of the eddy in front of the right deflector is located below the high velocity jet and the area occupied by downwelling of the water is larger. The absence of a baffle wall allows propagation of the high velocity jets significantly further (Figures 5(e) and (f)). However, the flow direction in the auxiliary bays is opposite to the main flow. This back flow reduces the size of the eddy in front of the right deflector and moves its center towards the deflector.

The velocity distributions in the left auxiliary bay (Figures 4(c) and (f)) are remarkably different with and without the baffle wall. Upstream of the baffle wall, the high

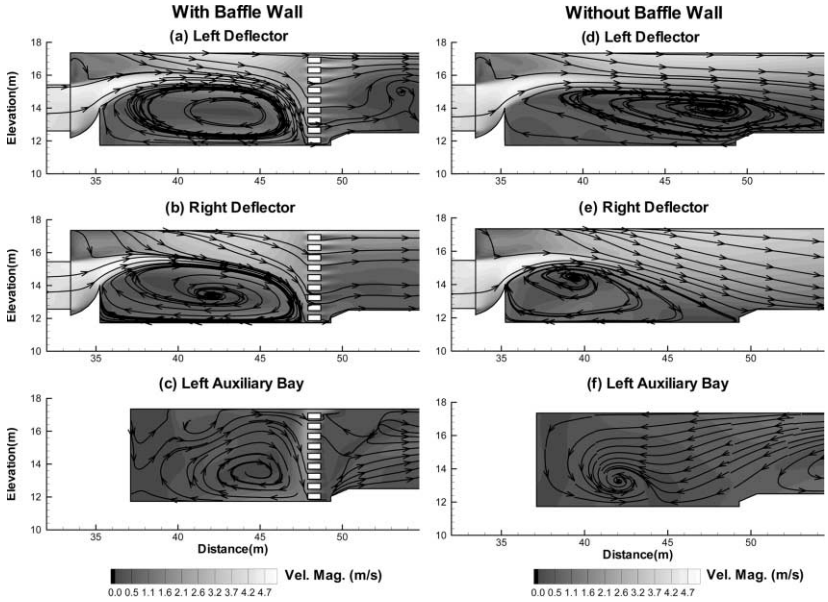

Figure 4 | Velocity distributions and streamlines at three vertical sections with (a–c) and without (d–f) the baffle wall.

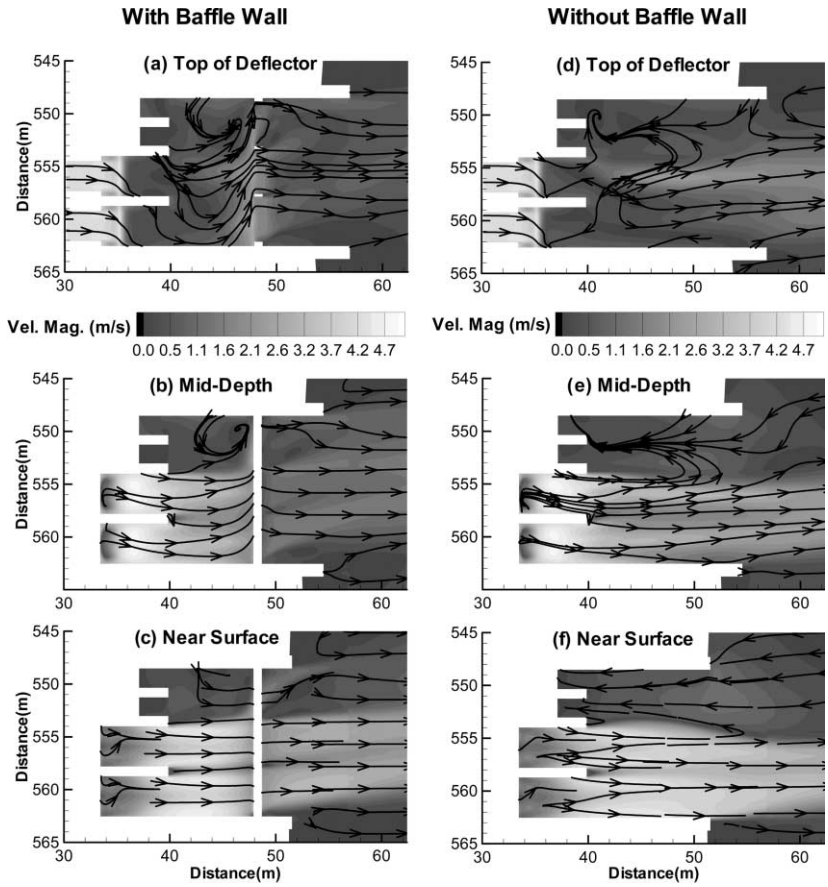

Figure 5 | Velocity distributions and streamlines in three horizontal planes with (a–c) and without (d–f) the baffle wall.

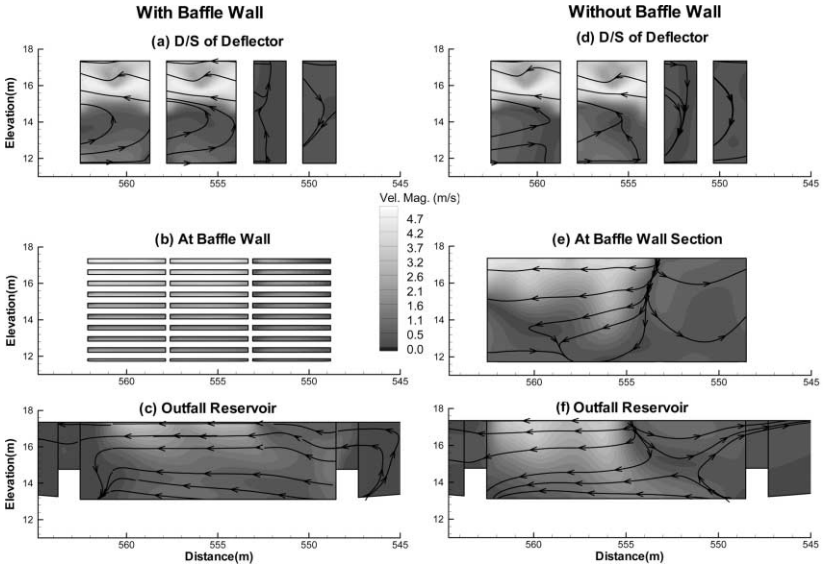

Figure 6 | Velocity distributions and streamlines in three transverse sections with (a–c) and without (d–f) the baffle wall.

velocity jets are deflected towards the auxiliary bays (Figures 5(a)–(c)), creating a relatively uniform velocity (in the vertical) on the upstream side of the baffle wall (Figure 4(c)). Upstream of the baffle wall, a large eddy occupies most of the auxiliary bay. Without the baffle wall, back flow occurs in the auxiliary bays. Similar return flow and flow convergence can be observed in Figures 5(d)–(f). These converging flows spread out laterally as indicated by diverging streamlines in Figures 6(e) and (f).

The effects of the baffle wall on outflow velocities can be visualized by comparing Figures 6(b) and (c) with Figures 6(e) and (f), respectively. With the baffle in place, the cross sectional area is smaller and the velocities are higher in the middle of the structure (Figure 6(b)). The cores of the high velocity jets are distinctly visible at the baffle wall (Figures 6(b) and (e)). As the jet propagates downstream, velocities in the jets decrease considerably. With the baffle wall, the two jets merge and the higher velocities are confined in the upper water column. Without the baffle wall, velocities at the outlet are higher and the core of the jet occupies a larger area. With and without the baffle wall, the maximum computed velocities at the outlet (Figures 6(c) and (f)) are 3.2 m/s and 3.5 m/s, respectively. The corresponding near-bed velocities are 0.9 m/s and 1.6 m/s. Thus, the baffle wall reduces the near-bed velocities, responsible for scouring the reservoir bed, by about 75%.

SUMMARY AND CONCLUSIONS

A 3D CFD model of an outfall structure discharging 55 m^3/s of cooling water into a reservoir by a power plant has been presented in this paper. The outfall structure, 23.2 m long, 16.5 m wide and 5.6 m high, is divided into four bays on the upstream side. Cooling water is conveyed to the structure by two 2.9 m diameter pipes. Two deflectors, formed by 2.1 m radius quarter cylinders, are at the downstream end of the inflow pipes. A baffle wall consisting of a large number of open slots is located at a distance of 15 m from the deflectors. The computational grid of the CFD model consists of 350,660 hexahedral cells, with cell sizes varying from 0.05–0.28 m. The adequacy of the computational grid in resolving the geometric and hydraulic features of the outfall structure was ascertained by comparing results with a coarse resolution CFD model.

A detailed characterization of the hydraulics of the outfall structure, with and without a baffle wall, has been performed. The results of the CFD model indicate that interaction of the high velocity inflow with the deflectors and baffle wall creates a complex flow field in the outfall structure. The high velocity jets are deflected towards the water surface by the deflectors. As a result, velocities are higher near the water surface. Initially, the jets bifurcate and then reattach near the outlet. The shear stress exerted by

the jets on the surrounding water creates eddies, dead flow zones and flow separations. The CFD model results indicate that maximum velocities of similar magnitude occur near the water surface for both configurations. However, the baffle wall is effective in reducing the near-bed velocities by approximately 75%. This study illustrates an efficient and cost effective method of investigating hydraulics of an outfall structure by using a 3D CFD model. The results of the model were used for optimizing the design of the outfall system at the power plant.

REFERENCES

Ali, K. H. M. & Karim, O. 2002 Simulation of flow around piers. *J. Hydraul. Res.* **40** (2), 161–174.

Brouckaert, C. J. & Buckley, C. A. 1999 The use of computational fluid dynamics for improving the design and operation of water and wastewater treatment plants. *Wat. Sci. Technol.* **40** (4–5), 81–90.

Computational Dynamics Ltd. 1999 *Methodology, STAR-CD Version 3.10*. Computational Dynamics Ltd., London, UK.

Greene, D. J., Hass, C. N. & Farouk, B. 2002 Numerical simulation of chlorine disinfection processes. *Wat. Sci. Technol.: Wat. Supply* **2** (3), 167–173.

Khan, L. A., Wicklein, E. D., Rashid, M., Ebner, L. L. & Richards, N. A. 2004 Computational fluid dynamics modeling of turbine intake hydraulics at a hydropower plant. *J. Hydraul. Res.* **42** (1), 61–69.

Lai, Y. G., Weber, L. J. & Patel, V. C. 2003 Nonhydrostatic three-dimensional model for hydraulic flow simulation. I: Formulation and verification. *J. Hydraul. Engng.* **129** (3), 196–205.

Lomax, H., Pulliam, T. & Zingg, D. 2003 *Fundamentals of Computational Fluid Dynamics*. Springer, Berlin.

Morvan, H., Pender, G., Wright, N. G. & Ervine, D. A. 2002 Three-dimensional hydrodynamics of meandering compound channel. *J. Hydraul. Engng.* **128** (7), 674–682.

Rodi, W. 1980 *Turbulence Models and Their Application in Hydraulics*. International Association for Hydraulic Research, Delft, The Netherlands.

Salaheldin, T. M., Imran, J. & Chaudhry, M. H. 2004 Numerical modeling of three-dimensional flow field around circular piers. *J. Hydraul. Engng.* **130** (2), 91–100.

Savage, B. M. & Johnson, M. C. 2001 Flow over ogee spillway: physical and numerical model case study. *J. Hydraul. Engng.* **127** (8), 640–649.

Stamou, A. I. 2002 Verification and application of a mathematical model for the assessment of the effect of guiding walls on the hydraulic efficiency of chlorination tanks. *J. Hydroinf.* **4** (4), 245–254.

Thomson, J. F., Soni, B. K. & Weatherill, N. P. 1999 *Handbook of Grid Generation*. CRC Press, Boca Raton, FL.

Wright, N. G. & Hargreaves, D. M. 2001 The use of CFD in the evaluation of UV treatment systems. *J. Hydroinf.* **3** (2), 59–70.

Yeung, H. 2001 Modelling of service reservoirs. *J. Hydroinf.* **3** (3), 165–172.